

RESEARCH REPORT

Harpalus (Pseudoophonus) rufipes* as a model to study cellular and humoral immune defence strategies in coleopteran species*F Cavaliere¹, P Brandmayr¹, PG Giulianini², ML Vommaro¹, A Giglio^{1*}**¹*Department of Biology, Ecology and Earth Sciences, University of Calabria, Rende, Italy*²*Department of Life Sciences, University of Trieste, Trieste, Italy**Accepted June 3, 2019***Abstract**

Carabids are of special interest as environmental quality assessment indicators of exposure to xenobiotic and for pest control. In agroecosystems, they can be exposed to a wide range of pathogens and environmental pollution exerting a stronger selection on their innate immune systems. Therefore, information on species-specific immunocompetence is necessary to complete the ecological framework of ground beetles. In this study, cellular and humoral responses were characterized in adults of *Harpalus (Pseudoophonus) rufipes* (De Geer, 1774) to define a baseline knowledge for future ecotoxicological studies. The circulating hemocytes were characterized by light and transmission electron microscopy and *in vivo* assay performed by injecting latex beads to identify phagocytizing hemocytes. Ultrastructural analyses revealed four morphologically distinct types of circulating hemocytes: prohemocytes, plasmatocytes, granular cells and oenocytoids. Differential hemocyte counts showed that plasmatocytes and granular cells were the most abundant circulating cell types and granular cells exhibited phagocytic activity following immune challenge with latex beads. Mitotic figures and non-differentiated hemocytes observed under light microscopy indicate a continuous cell turnover in the hemolymph. Melanotic nodules found 2h after the immune challenge were formed to immobilize the latex beads. Phenoloxidase (PO) assays revealed an increase of basal PO activity in hemolymph after immune system activation with lipopolysaccharide (LPS). However, the LPS-stimulated adults showed no significant variation in the lysozyme-like enzyme activity in hemolymph. Based on these results, *H. rufipes* displays a rapid, non-specific immune response involving cellular and humoral effectors that both sequester and clear pathogens.

Key Words: hemocytes; ultrastructure; phagocytosis; nodulation; phenoloxidase; lysozyme; carabid beetles**Introduction**

Evolutionary and ecological studies on insect immunocompetence have provided evidence that the ability to resist disease is a life history trait that depends upon biotic and abiotic ecological factors including habitat quality, resource availability, life cycle and gender (Moreno-García *et al.*, 2014). Ecological inputs generate high species-specific diversity in both constitutive and induced immune responses (Schmid-Hempel, 2003, 2005; Sadd and Schmid-Hempel, 2009; Schulenburg *et al.*, 2009). Thus, information on the strength, speed and specificity in recognizing and processing pathogens

is of great interest in an increasing numbers of species for controlling pests (Bulmer *et al.*, 2009; Hillyer and Strand, 2014) as well as for reducing mortality of beneficial insects (James and Xu, 2012).

The innate immune system of insects includes cellular and humoral immune defences, which provide an active barrier against pathogens (Hillyer, 2016). Hemocyte-mediated immune responses include phagocytosis, nodule formation and melanotic encapsulation (Ribeiro and Brehélin, 2006; Strand, 2008). Phagocytic activity of hemocytes is a fundamental innate immune mechanism used to recognize (Ottaviani, 2005; Lamprou *et al.*, 2007; Rosales, 2011), ingest and kill pathogens or to remove apoptotic cells (Marmaras and Lampropoulou, 2009; Tsakas and Marmaras, 2010). Nodulation and encapsulation are cellular immune responses against bacteria and parasites too large for phagocytosis (Gillespie and *et al.*, 1997; Satyavathi *et al.*, 2014; Hillyer, 2016). The humoral

Corresponding author:

Anita Giglio
 Department of Biology
 Ecology and Earth Science
 University of Calabria
 Via P. Bucci, I-87036 Rende
 E-mail: anita.giglio@unical.it

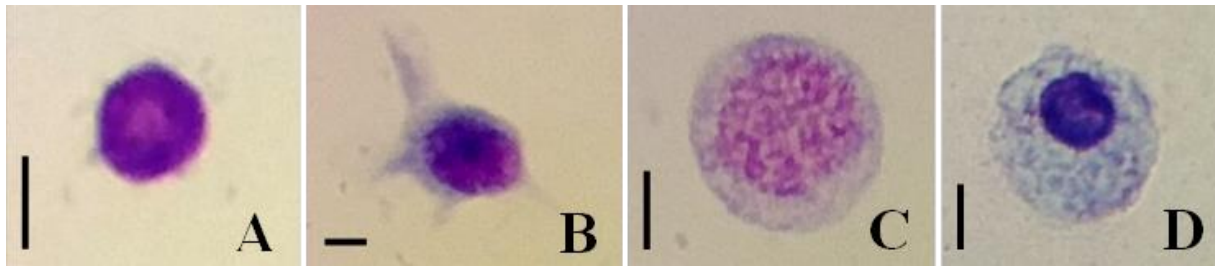


Fig. 1 Circulating hemocytes in adults of *H. rufipes*, Giemsa stained for light microscopy observations. (A) Prohemocyte. (B) Plasmatocyte. (C) Granular cell. (D) Oenocytoid. Scale bar: 5 μ m

immune response involves synthesis of antimicrobial peptides (AMPs), phenoloxidase (PO) enzymatic cascade and production of reactive oxygen and nitrogen species. AMPs are secreted proteins with lytic activity such as lysozyme (muramidase) that play an important role in immune defence by performing a hydrolytic action against peptidoglycan of Gram positive cell walls (Ratcliffe *et al.*, 1985; Hultmark, 1996; Gillespie *et al.*, 1997; Nappi and Ottaviani, 2000; Callewaert and Michiels, 2010; Wagner *et al.*, 2015). It is present constitutively at a very low level in the hemolymph and increases upon challenge. The proPO-activating system comprises a complex cascade of serine proteases allowing the conversion of proPO to PO (Marmaras and Lampropoulou, 2009; González-Santoyo and Córdoba-Aguilar, 2012). The PO enzymatic system can be triggered by pathogen cell surface molecules such as β -1,3 glucans from fungal cell walls and lipopolysaccharides (LPS) and peptidoglycans from microbial cells. This PO enzymatic complex converts phenols to quinones that subsequently polymerize to form melanin (González-Santoyo and Córdoba-Aguilar, 2012). Melanin is involved in physiological processes such as melanisation and sclerotization of cuticle, which improves its ability to act as a physical barrier to invading parasites and pathogens (Wilson *et al.*, 2001; Dubovskiy *et al.*, 2013). Moreover, melanogenesis exerts antimicrobial activity in tissue repair and pathogen sequestration (wounding, clotting, melanotic encapsulation, production of cytotoxic molecules) (Söderhäll *et al.*, 1994; Marmaras *et al.*, 1996; Nappi and Vass, 2001; Nappi and Christensen, 2005; Cerenius *et al.*, 2008; González-Santoyo and Córdoba-Aguilar, 2012; Hillyer, 2016).

Harpalus (Pseudoophonus) rufipes (De Geer, 1774) is a generalist predator that acts as a biological control agent of pests, feeding on seeds (Honek *et al.*, 2003, 2005, Saska *et al.*, 2008, 2010; Talarico *et al.*, 2016; Reshetniak *et al.*, 2017) and invertebrates (Holland, 2002; Monzó *et al.*, 2011; Brygadyrenko and Reshetniak, 2014) in different crops (Holland, 2002; Miñarro *et al.*, 2009; Monzó *et al.*, 2011). A previous study demonstrated that this beneficial species is sensitive to agricultural management practices, especially the use of herbicides (Cavaliere *et al.*, 2019). In spite of their ecological role and sensitivity as exposure

indicators, no data are available concerning the cellular and humoral effectors involved in recognition and immobilization of pathogens in the hemolymph of *H. rufipes*.

To evaluate the immune function of *H. rufipes* adults, we morphologically characterized circulating hemocytes by light and transmission electron microscopy and measured a set of the most common immune markers used in ecological and evolutionary studies to define the constitutive and inducible immune defences of insects. Phagocytosis after *in vivo* artificial non-self challenge with latex beads was analysed as a general measurement of the cellular immune response. The basal and total PO and lysozyme-like enzyme activities after *in vivo* lipopolysaccharide challenge were investigated as immunity markers of the humoral defences.

Material and methods

Insects

Harpalus rufipes adults were collected using *in vivo* pitfall traps (plastic jars 9 cm in diameter) containing fruit as an attractant. The sampling was performed in a wheat field of 5 ha located on the Sila Mountain at 1240 m a.s.l., (39°16'58.05"N, 16°38'43.26"E, Società Cooperativa Orti dei Monti, Torre Garga Farm, San Giovanni in Fiore, Calabria, Southern Italy) in spring 2018.

In the laboratory, beetles were kept in groups in 10 L plastic boxes filled to a depth of 6 cm with soil from the capture site. The specimens were reared for one week before hemolymph collection with a light regime of L15:D9, 60% r.h. and at a day/night temperature of 24/20 °C. Adults fed on homogenized meat and fruit *ad libitum*. The experimental design was conducted in accordance with all applicable government and institution laws and rules.

Immune challenges

Lipopolysaccharide

To assess the immune response to lipopolysaccharide (LPS) treatments, we used a 10 μ L Hamilton syringe to inject 4 μ L of LPS (0.5 mg/mL phosphate buffer) from *Escherichia coli* 0127:B8 (Sigma-Aldrich, L3129) into the hemocoel of cold anesthetized adults at the dorsal level of the 7th abdominal tergite. Twenty-four hours after injection, the hemolymph was collected by

puncturing cold anaesthetized adults at the ventral level of the pro-mesothorax articulation with a 29-gauge needle. A pool of 10 μL of hemolymph was collected from three specimens, immediately transferred into 90 μL ice-cold sterile phosphate-buffered saline (PBS, 10mM; Sigma-Aldrich) and centrifuged at 1700g for 5 min at 4 °C. Parallel controls were run with a group of non-injected insects. The cell-free hemolymph obtained as supernatant has been collected and stored at -20 °C prior to measure PO and lysozyme-like enzyme activities.

In vivo phagocytosis

To assess the ability of hemocytes to phagocytize, we used a 10 μL Hamilton syringe to inject 4 μL of carboxylate-modified polystyrene latex beads (0.9 μm in diameter, aqueous suspension, 10% solids content, Sigma-Aldrich) diluted 1:10 in 0.15 M sterile PBS into the hemocoel as described above. After injection of latex beads, adults were incubated for 2 hours before microscopy analyses were performed. Parallel assays were run with non-injected animals as control.

Light and transmission electron microscopy

To estimate the number of circulating cells per μL of hemolymph (total hemocyte counts, THCs) without distinction of morphology and function, 3 μL of hemolymph were collected from control animals by puncturing cold anaesthetized adults at the ventral level of the pro-mesothorax articulation with a 29-gauge needle. Hemocytes were counted in a Bürker's hemocytometer (Carlo Erba, Italy) without dilution and observed with light microscopy (LM) (Zeiss Primo Star) at 400x magnification. THC was expressed as the number of cells (mean \pm SE) per mL of hemolymph.

The differential hemocyte count (DHC) was calculated as the relative percentage of different cellular morphotypes circulating in hemolymph for each sample. The hemolymph (3 μL for each beetles) was collected (as described above) from control (n= 14) and latex bead treated (n= 12) beetles and mixed with 5 μL of PBS, spread on a poly-L-lysine coated slide and dried at room temperature for approximately 30 s. During this time, the hemocytes adhered to the glass. Cells were then fixed in methanol for 10 min. After natural air-drying of the fixative, hemocytes were stained with Giemsa (1:20 in distilled water) for 5 min and slides were rapidly washed with distilled water. We analysed approximately 200 cells per slide with light microscopy (Zeiss Primo Star) at 1000x magnification.

For transmission electron microscopy, a pool of 20 μL of hemolymph was collected from five specimens of both latex bead treated and non-injected control groups. Beetles were cold anaesthetised and the last two abdominal segments laterally torn; a 29-gauge needle was inserted in the neck membrane and sterile phosphate-buffered saline (PBS, Sigma) slowly injected. When the first drop of hemolymph coming out from abdomen of the beetles, it was collected in a microcentrifuge tube containing fixative consisted of 2.5 % glutaraldehyde, 1 % paraformaldehyde and 7.5 %

picric acid in 0.1 M phosphate buffer, pH 7.4, with 1.5% sucrose for 2 h at 4 °C. Samples have then centrifuged at 1700g for 5 min at 4 °C and the supernatant removed. Pellets were rinsed in phosphate buffer, post-fixed with 1% osmium tetroxide in 0.1 M phosphate buffer for 2 h at 4 °C and rinsed in the same buffer. Dehydration in a graded acetone series was followed by embedding in Epoxy resin (Sigma Aldrich). Ultrathin sections, cut with a PT-PC PowerTome Ultramicrotome (RMC Boeckeler), were examined with a Jeol JEM 1400 Plus electron microscope (Microscopy and Microanalysis Centre, CM2, Laboratory of Transmission Electron Microscopy - University of Calabria, Italy) at 80 kV. Measurements of hemocytes were taken with Image-Pro Plus version 4.5 software (Media Cybernetics) on digitized images and processed as mean \pm standard error.

Enzymatic assays

Phenoloxidase enzyme activity

Phenoloxidase (PO) enzyme activity was measured in cell-free hemolymph of both untreated and LPS-injected (treated) animals. Basal PO activity was assayed spectrophotometrically as the formation of dopachrome from 3,4-dihydroxy-L-phenylalanine (L-DOPA, Sigma-Aldrich). To determine the basal PO, 10 μL of hemolymph-buffer solution, collected as described above, was mixed with 90 μL of L-DOPA (3 mg/mL in PBS) in a microtiter plate. To measure the total PO enzyme activity, 10 μL of the hemolymph-PBS mixture was added to 5 μL of bovine pancreas alpha-chymotrypsin (5 mg/ml PBS, Sigma), and incubated for 5 min at room temperature to activate PO from its inactive zymogen. Subsequently, 85 μL of L-DOPA was added to the solution. The change in absorbance was recorded at 492 nm and 25 °C for 30 min in 1 min intervals using a plate reader (Sirio S, SEAC). All samples were assayed in duplicate. The enzyme activity was measured as the slope (absorbance vs time) of the reaction curve during the linear phase of the reaction (V_{max} value; between 0 and 30 min after the reaction began). The slope of the reaction curve at V_{max} was plotted as absorbance per μL of hemolymph per min for specimens from each group.

Lysozyme-like enzyme activity

Lysozyme-like activity was assayed by turbidometric changes in the cell-free hemolymph based on Adamo (2004). The decrease in absorbance over time indicates that lysozyme degrades cell walls of the lysozyme-sensitive Gram-positive bacterium *Micrococcus lysodeikticus*. Ten μL of hemolymph-PBS mixture (collection described above) from untreated and LPS-injected (treated) animals was loaded into the wells of a 96-well microplate and mixed with 190 μL of a *M. lysodeikticus* (strain ATCC 7468, DSMZ) cell wall suspension (approximately 1.6×10^8 cell/mL of cold PBS). The turbidity reduction in the wells were read on a plate reader (Sirio S, SEAC) at 450 nm and 25 °C for 45 min in 5 min intervals. All samples were assayed in duplicate. The enzyme activity was reported as the change in absorbance (absorbance

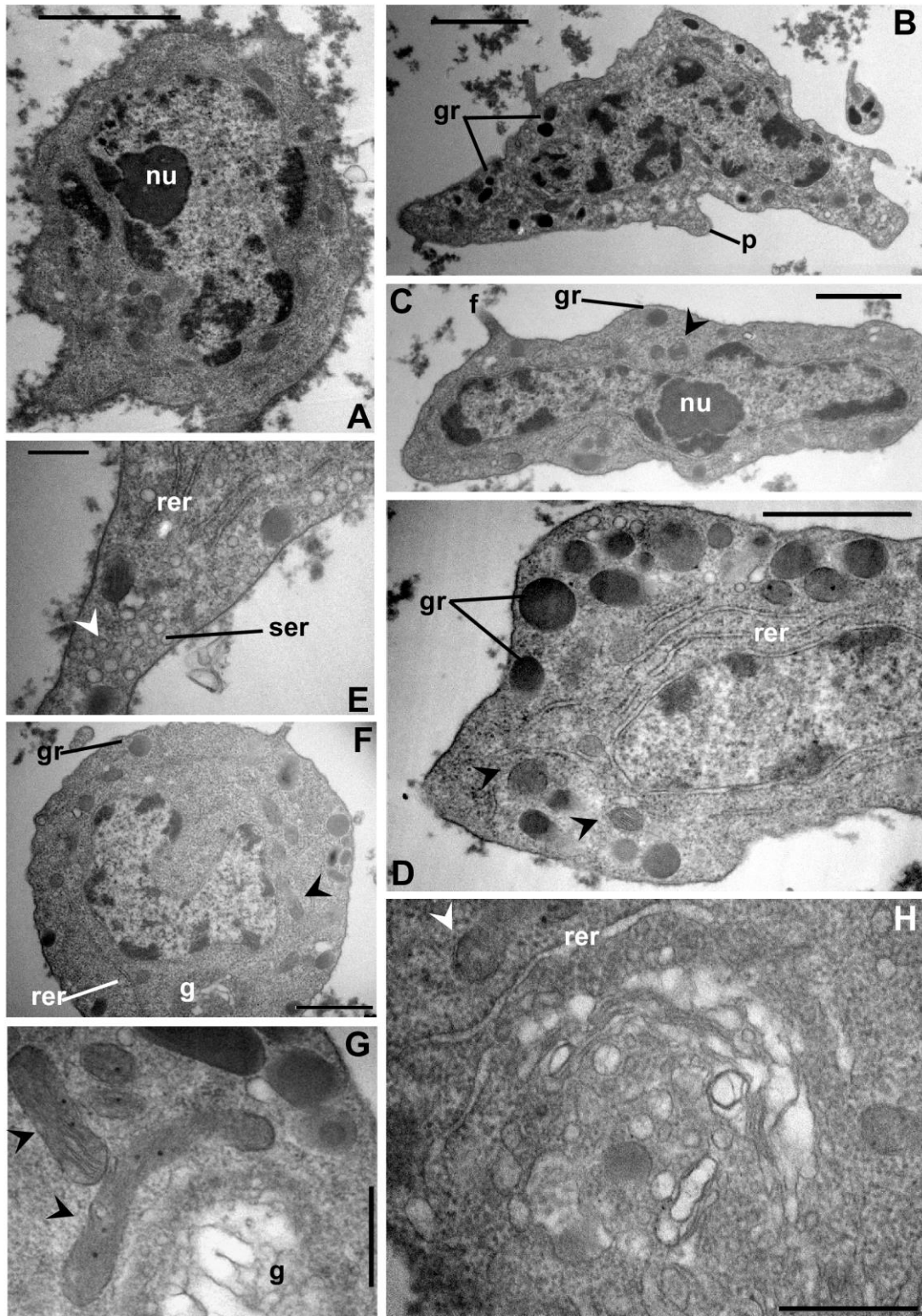


Fig. 2 Transmission electron microscopy of *H. rufipes* hemocytes, control. (A) Prohemocyte shows a prominent nucleolus (nu) and high nucleus/cell surface ratio. (B-D) Longitudinal sections of plasmatocytes. Numerous small electron dense granules (gr) and mitochondria (arrowheads) are present in the cytoplasm. The plasmatic membrane is irregular and prolonged in filopodia (f) or pseudopodia (p). The rough endoplasmic reticulum (rer) is arranged in large cisternae (D-E) surrounding a heterochromatic nucleus with an evident nucleolus (nu) (C). (E) Higher magnification of the plasmatocyte showing vesicles of smooth endoplasmic reticulum (ser) in the cytoplasm. (F) Cross section of a young plasmatocyte. The cytoplasm contains a low concentration of rough endoplasmic reticulum (rer), free ribosomes, mitochondria, and Golgi complex (g). (G) Detail (from plasmatocyte in Fig. D) of mitochondria with evident cristae. (H) Higher magnification showing saccotubular compartment of Golgi complex. Scale bar: 500 nm (E,G,H) 1 μ m (C,D,F), 2 μ m (A,B)

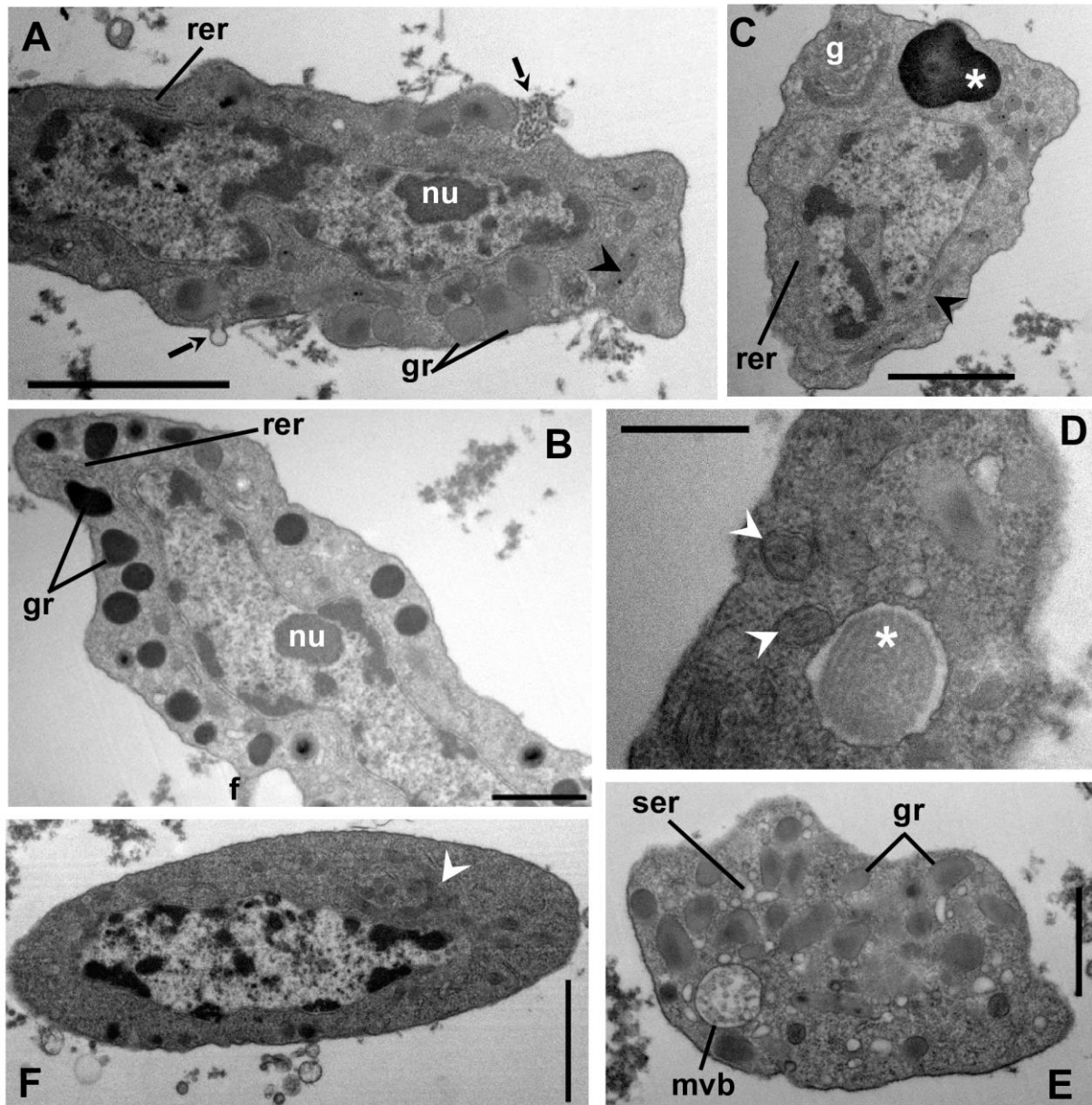


Fig. 3 Transmission electron microscopy of *H. rufipes* hemocytes, control. (A-B) Granular cell, longitudinal section. Within the cytoplasm are found characteristic large electron dense granules (gr), mitochondria (arrowhead) and rough endoplasmic reticulum (rer) are evident in the cytoplasm. At the level of plasmatic membrane, endo and exocytosis activities are evident (black arrow). The irregular shaped plasmatic membrane is also interrupted by filopodia (f). The nucleus is lobate with densely packed heterochromatin adjacent to the nuclear envelope. (C) Granular cell, cross-section. Golgi complex and a large electron-dense vesicle (asterisk) are evident. (D) Granular cell, detail of the cytoplasmic compartment. The high magnification shows mitochondria (arrowhead) and a granule (asterisk) containing tubular elements. (E) Detail of cytoplasmic region of granular cell showing a multivesicular body (mvb) limiting intraluminal vesicles and many vesicles of smooth endoplasmic reticulum (ser). (F) Oenocytoid, transversal section shows the peculiar regular round profile and the homogenous cytoplasm. Scale bar: 500 nm (D), 1 μ m (B,E), 2 μ m (A,C,F)

vs time) of the reaction curve during the linear phase of the reaction (V_{max} value; between 5 and 15 min after the reaction began). The slope of the reaction curve at V_{max} was plotted as absorbance per μ L of hemolymph per min, for both LPS-treated and control adults. Standards of enzyme activity

were made using lysozyme from chicken egg whites (Sigma) and a suspension of *M. lysodeikticus* as substrate. The standards were incubated and recorded simultaneously with the hemolymph samples to confirm that the assay progressed as expected (i.e. absorbance values decreasing).

Statistical analyses

Statistical analyses were performed using R version 3.0.1 software (R Development Core Team 2013). All immune parameters were measured (mean \pm SE) and compared between challenged and control adults. The differences were assessed by non-parametric statistics, *i.e.*, Welch two sample t-test sum test, followed by post-hoc Wilcoxon rank sum test pairwise comparisons, with Bonferroni correction since the null hypothesis of the Bartlett test could not be rejected.

Results

Hemocyte types and morphology

The total number of circulating hemocytes in hemolymph of *H. rufipes* was $4.4 \pm 0.2 \times 10^6$ cells/mL (n=15). Four morphological types of circulating cells were identified for their size, morphology and dye-staining properties: prohemocytes (Figs 1A and 2A), plasmatocytes (Figs 1B and 2B-H), granular cells (Figs 1C and 3A-E) and oenocytoids (Figs 1D and 3F).

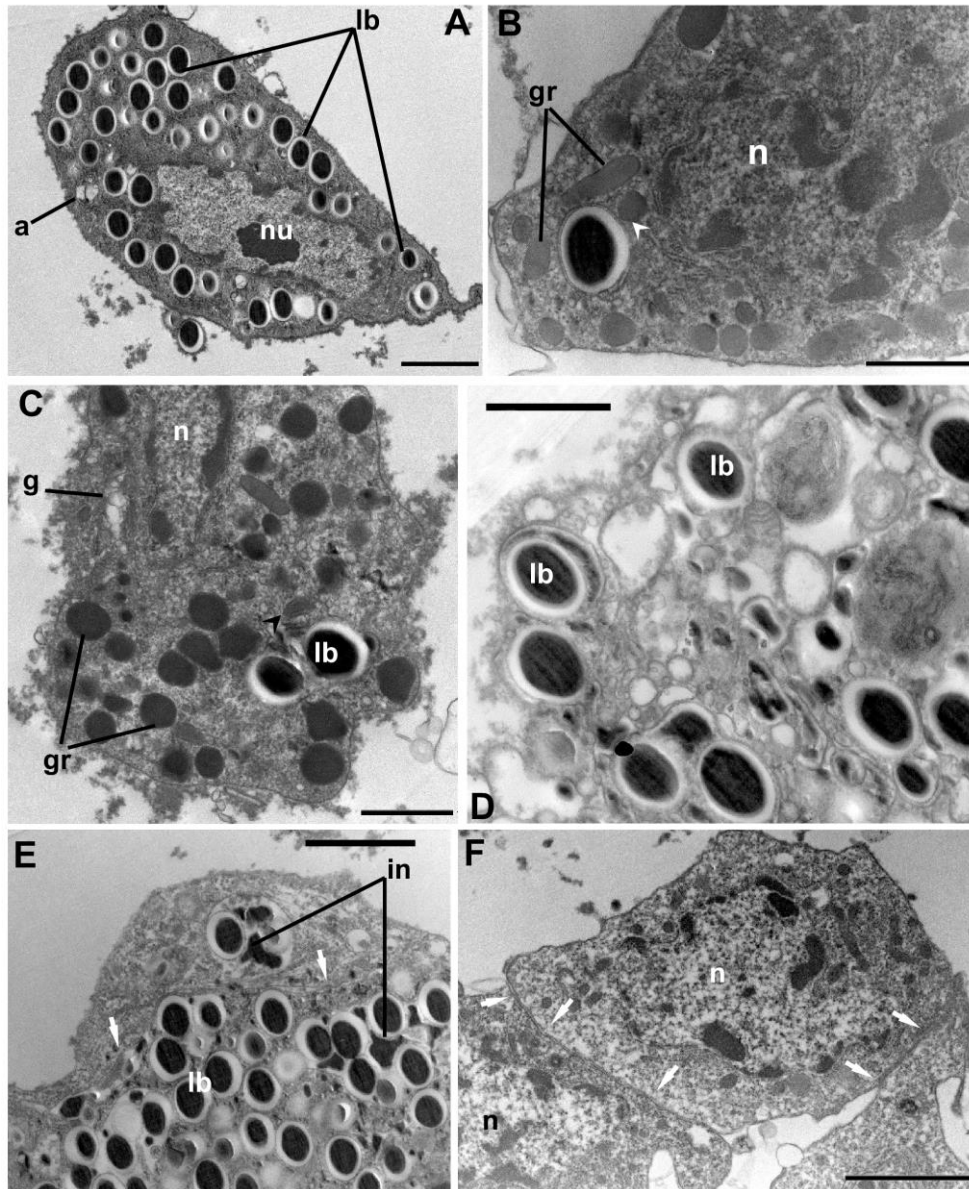


Fig. 4 Transmission electron microscopy of *H. rufipes* hemocytes 2 h after *in vivo* artificial non-self-challenge with latex beads. (A) Granular cell phagocytized a large amount of beads and phagosomes containing clusters or single latex beads. (B) Higher magnification of cytoplasm. Granules (gr) fusing with the phagosome are evident demonstrating their role as primary lysosomes. (C) Detail of cytoplasmic region shows phagosome containing latex beads (lb) and large electron dense granules (gr). (D) Phagocytizing granular cells show cellular fragmentation and membrane blebs suggesting an apoptotic process. (E) Detail of aggregate phagocytizing granular cells becoming to secrete melanised inclusions (in). (F) Detail of early aggregation of plasmatocytes in nodule formation. a: autophagosome, arrowheads: mitochondria, white arrows: septate junction, g: Golgi complex, n: nucleus, nu: nucleolus. Scale bar: 1 μ m (B,C,D), 2 μ m (A,E,F)

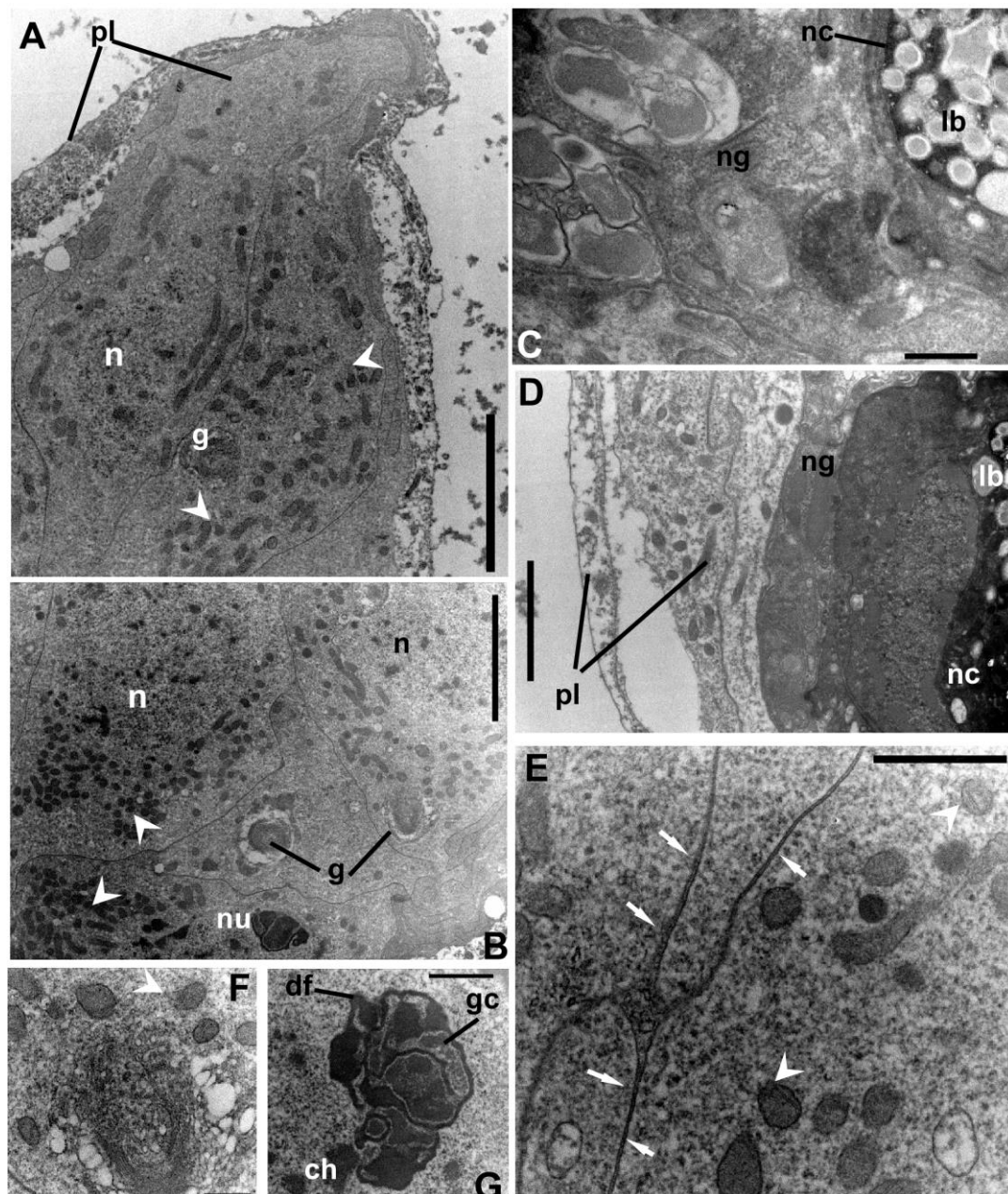


Fig. 5 Transmission electron microscopy of nodules 2 h after *in vivo* artificial non-self-challenge with latex beads. (A-B) In the outer region of the nodule, plasmacytes are aggregated around the surface of the nodule. Golgi complexes and mitochondria (arrowheads) are evident in the cytoplasm. The euchromatic nucleus (n) indicates a high transcription activity. (C-D) Mature nodules show a necrotic core (nc) consisting of latex beads (lb), an extensive melanised matrix and necrotic granular cells (ng) ensheathed by flattened plasmacytes (pl). (E) Detail of cytoplasm showing septate junction (white arrows) between adherent plasmacytes. (F) Detail of Golgi complex. (G) Higher magnification of nucleolus. Dense fibrillar (df) and granular (gc) components are evident. ch: chromatin. Scale bar: 500 nm (C,F), 1 μ m (E,G), 2 μ m (D), 5 μ m (A,B)

Prohemocytes are the smallest cells found in the hemolymph and display a spherical profile (5 μ m x 6 μ m in diameter) and an intense blue colour (basophilic) after Giemsa staining (Fig. 1A). The nucleus almost fills the cell and the nucleus/cell surface ratio is 0.7 in section (Fig. 2A). A well-developed rough endoplasmic reticulum and small mitochondria occur in the cytoplasm.

Plasmacytes are irregularly shaped cells with a maximum diameter up to 13 μ m (Figs. 2B and C). The cytoplasm looks basophilic after Giemsa staining (Fig. 1B) and ultrastructural analyses show numerous electron dense granules with a mean diameter of $0.34 \pm 0.01 \mu$ m (N=43) (Figs 2B-D). The nucleus is large 7 μ m x 2 μ m, lobed and euchromatic with a prominent large nucleolus (Fig.

2C). The rough (Figs 2D, F and H) and smooth (Fig. 2E) endoplasmic reticulum and the Golgi complexes (Figs 2G,H) are well developed. Numerous elongated mitochondria with tubular cristae are observed (Fig. 2G). The plasma membrane exhibits irregular pseudopodia (Fig. 2B) and filopodia (Fig. 2C).

Granular cells have an elliptical profile with a maximum diameter up to 13 μm (Figs. 3A-D). The nucleus is large approximately 6.35 μm x2.6 μm , lobed and euchromatic with a prominent large nucleolus (Fig. 3A-C). After Giemsa staining, they exhibit a homogeneous cytoplasm containing acidophilic granulations (Fig.1C). These granules are variable in electron density with a round irregular to elliptical profile and have a mean diameter of 0.55 \pm 0.02 μm (n=58) (Figs. 3A-D and E). In some cases, structured granules (Fig. 3D) contains tubular elements. The cytoplasm contains rough endoplasmic reticulum, Golgi complexes and elongated mitochondria (Figs 3A-C). Multivesicular bodies (MVBs, about 1 μm in diameter) were clearly identifiable (from 2 to 4 MVBs per section) adjacent to the plasma membrane trapping numerous intraluminal vesicles (69 \pm 12 nm in diameter, n =22) (Fig. 3E).

Oenocytoids are rare compared to the other cell types encountered in the hemolymph (Fig. 3F). They are round cells, approximately 16 μm x 23 μm in diameter, characterized by an eccentric nucleus. The cytoplasm has few organelles, although small oval mitochondria, free ribosomes, numerous polysomes and a rough endoplasmic reticulum are sometimes present. After Giemsa staining, the oenocytoids exhibit a mild basophilic cytoplasm and a strong basophilic nucleus (Fig. 1D).

In vivo phagocytosis assay

After 2 h *in vivo* artificial non-self-challenge with latex beads, granular cells mounted a strong and rapid phagocytic response. They present up to 40 phagocytized beads within the cytoplasm and become enlarged (Figs 4A, B and D). Phagocytizing cells occurred as either isolated (Figs 4A, B and C) or aggregate cells (Fig. 4E). Granules fusing with a phagosome are evident, demonstrating their role as primary lysosomes (Fig. 4B). Extensive plasma

membrane blebbing followed by separation of cell fragments into apoptotic bodies were found in some granular cells having their cytoplasm filled with a high numbers of latex beads (Fig. 4D). Melanised nodules are found in the hemolymph entrapping a large number of beads 2h after the challenge (Figs 5A-D). Each nodule has a necrotic core (Figs 5C and D) consisting of latex beads embedded in an extensive melanised matrix and necrotic granular cells (Fig. 5D) covered by a layer of flattened plasmatocytes (Figs 4F, 5A, B). Septate junctions are evident between plasmatocytes that aggregate around the surface of the nodules (Figs 4F; 5A, B, and E). Moreover, numerous mitochondria and well-structured Golgi complexes are present in the cytoplasm (Figs 5A, B and F) as well as a large euchromatic nucleus with an evident nucleolus (Figs 5B and G).

Differential hemocyte counts (DHCs)

The DHCs performed in control beetles showed that plasmatocytes (67.15 \pm 2.52 %) and granular cells (29.32 \pm 2.35 %) are the main circulating hemocyte types, while prohemocytes (0.52 \pm 0.11 %) and oenocytoids (0.73 \pm 0.02 %) are rare in hemolymph (Table 1). After *in vivo* artificial non-self-challenge with latex beads, the relative percentage of granular cells (82.74 \pm 2.54 %; Wilcoxon rank sum test, $p= 1.74310^{-5}$) increases significantly in hemolymph and 54.31 \pm 2.88 % of them are phagocytizing cells. Moreover, a significant decrease in the relative percentage of plasmatocytes (12.38 \pm 2.21 %; Wilcoxon rank sum test, $p= 2.071 \times 10^{-7}$) and oenocytoids (0.16 \pm 0.05 %; Wilcoxon rank sum test, $p= 0.00797$) are recorded. No significant differences are remarked in prohemocytes between control and latex-treated beetles (Wilcoxon rank sum test, $p = 0.1725$).

In the DHCs, cells with intermediate features (Figs 2C, 3A) and hemocytes showing features of mitotic process (Figs. 6A-E) are also observed in both control and latex bead treated specimens ("Not determined" group in Table 1). However, the increase of their relative percentage from 2.28 \pm 0.37 % (ctrl) to 4.44 \pm 0.95 % (latex) of circulating hemocyte after latex bead challenge is not significant (Wilcoxon rank sum test, $p = 0.4105$).

Table 1 Relative percentages of circulating hemocyte types after latex bead challenge (latex; n = 12) compared with the non-injected (ctrl; n = 14) beetles

	Prohemocytes	Plasmatocytes	Granular cells	Phagocytizing	Oenocytoids	Not determined
ctrl	0.52 \pm 0.11	67 \pm 2.52	29.32 \pm 2.35	-	0.73 \pm 0.15	2.28 \pm 0.37
latex	0.28 \pm 0.11	12.38 \pm 2.21***	82.74 \pm 2.54***	54.31 \pm 2.88	0.16 \pm 0.08**	4.44 \pm 0.95

Note. Values are expressed as mean percentage \pm standard error; significance ascribed as ** p -value < 0.01 and *** p -value < 0.001 versus control

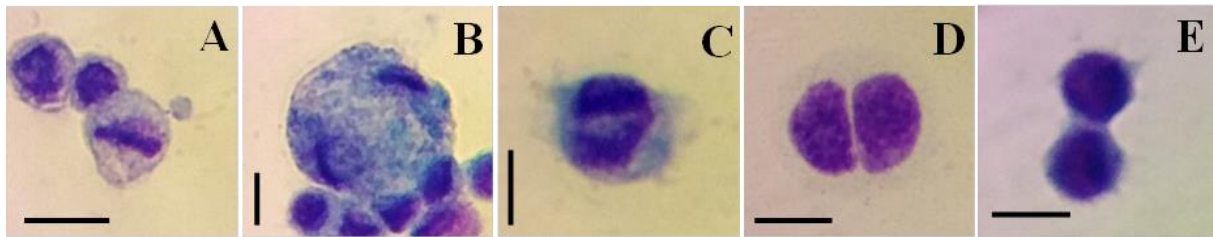


Fig. 6 Mitotic hemocytes in adults of *H. rufipes* Giemsa stained for light microscopy observation. (A) Metaphase hemocyte. (B) Anaphase. (C and D) Telophase. (E) Cytokinesis. Scale bar: 10 μ m

PO activity

Plasmatic basal PO activity was significantly higher (Wilcoxon rank sum test, $p = 0.01828$) in the LPS-treated adults (0.007 ± 0.002 Abs/ μ L/min; $n=11$) than that of untreated ones (0.002 ± 0.0005 Abs/ μ L/min; $n=18$; Wilcoxon rank sum test) (Fig. 7). No differences were observed in the plasmatic total PO activity (Wilcoxon rank sum test, $p = 0.6109$) between LPS-treated (0.005 ± 0.002 Abs/ μ L/min; $n=11$) and untreated (0.005 ± 0.0007 Abs/ μ L/min; $n=18$) specimens.

Lysozyme-like enzyme activities

The baseline lytic activity of hemolymph was not significantly higher (Wilcoxon rank sum test, $p = 0.1132$) in the LPS-treated adults (0.0012 ± 0.0003 Abs/ μ L/min; $n=13$) compared with untreated adults (0.0008 ± 0.0003 Abs/ μ L/min; $n=18$) (Fig. 7).

Discussion

In the current study, we provide the first description of the immunocompetence in the generalist predator *H. rufipes*. Based on light microscopy observations and ultrastructural analyses, we characterized four different types of circulating hemocytes: prohemocytes, plasmatocytes, granular cells and oenocytoids. The DHCs showed that plasmatocytes and granular cells are the most abundant circulating hemocytes. According to previous study (Ribeiro and Brehélin, 2006; Martins and Ramalho-Ortigao, 2012), circulating oenocytoids are large cells with a low nuclear to cytoplasmic ratio. The THC levels are in agreement with previous studies on circulating hemocytes of other Coleoptera species such as *Carabus lefebvrei* (12×10^6 cells/mL; Giglio *et al.*, 2008), *Rhynchophorus ferrugineus* ($3,85 - 5,2 \times 10^6$ cells/mL; Manachini *et al.*, 2011), *Dicladispa armigera* ($5,9 \times 10^6$ cells/mL; Phukan *et al.*, 2008). Morphology and function of hemocytes have been extensively investigated in insects. However, it lacks a unified terminology to indicate types and little is known about coleopteran species. Distinct classes such as prohemocytes, plasmatocytes, granular cells, coagulaocytes, oenocytoides and spherulocytes are identified in hemolymph of Tenebrionidae (Zhao and Wang, 1992), Coccinellidae (Firlej *et al.*, 2012), Curculionidae

(Manachini *et al.*, 2011), Melolonthidae (Akai and Sato, 1979; Gupta, 1979), Scarabeidae (Giulianini *et al.*, 2003) and Chrysomelidae (Phukan *et al.*, 2008). The low number of cellular subpopulations and hemocytes with intermediate feature and mitotic cells identified in *H. rufipes*, indicate proliferation and differentiation activities in circulating hemocytes of the adult stage. Further investigation can clarify if new circulating hemocytes in *H. rufipes* derive from germinal cells named prohemocytes and perform separate functions (Ottaviani, 2005; Strand, 2008; Hillyer, 2016) or arise from replication of mature granulocytes such as in mosquitoes (King and Hillyer 2013). Besides, morphotype has the ability to turn into another type as observed *in vitro* in plasmatocytes of *Periplaneta americana*, *Galleria mellonella* and *Tenebrio molitor* (Gupta and Sutherland, 1966) and in prohemocytes of *Bombyx mori* (Yamashita and Iwabuchi, 2001).

From an evolutionary ecology perspective, the immunocompetence of a species is a plastic life trait with costs of both maintenance and activation. Ecological factors influence the diversity and complexity of the cellular and humoral immune responses among different taxa exposed to a wider range of pathogens exerting stronger selection on the immune system. We performed immune challenges with latex beads and LPS to test separately the specificity of the cellular and humoral immune response in *H. rufipes*. Our results indicate that the dynamics of cellular and humoral responses in this species are highly adapted to maximize fitness. *H. rufipes* engages a rapid, non-specific constitutive immune response to fight off pathogens. Phagocytosis is the primary, rapid, non-specific, constitutive response of hemocytes to small particles such as bacteria. Granular cells and plasmatocytes have been reported to be the predominant phagocytic cell in insects (Gillespie *et al.*, 1997). Plasmatocytes carry out phagocytosis in Diptera (Lemaitre and Hoffmann, 2007; Govind, 2008; Hillyer and Strand, 2014; Honti *et al.*, 2014) and Lepidoptera (Ribeiro and Brehélin, 2006). Granular cells phagocytose pathogens in the larval stage of the coleopteran *Allomyrina dichotoma* (Hwang *et al.*, 2015). Furthermore, granular cells work together with other cell types to perform phagocytosis, oenocytoids in *Cetonischema aeruginosa* (Drury) larvae (Giulianini

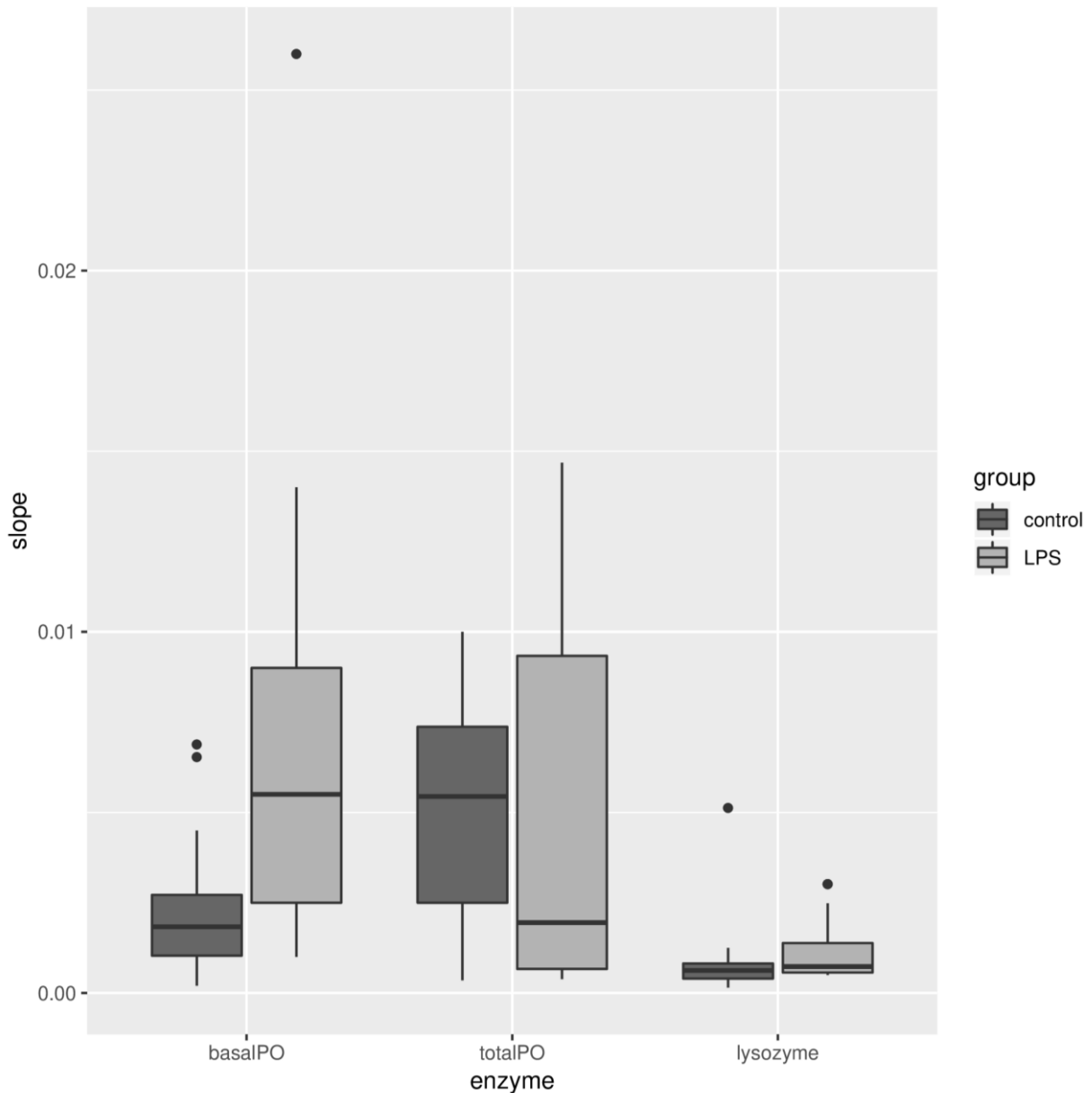


Fig. 7 The basal and total PO activities and lysozyme-like enzyme activity in non-injected (control) adults and treated one with LPS for 24 h. The enzyme activity (slope) was recorded as absorbance units for μL of hemolymph per min. The box represents the interquartile range (IQR = Q3 - Q1) and bars represent first (Q1, top) and third quartiles (Q3, bottom) of enzyme activity values from untreated and LPS-treated beetles. The central horizontal black line indicates the median. The ends of dashed lines (ends of the whiskers) represent the lowest (minimum) datum and the highest (maximum) datum

et al., 2003) or plasmatocytes in the larvae of red palm weevil *Rhynchophorus ferrugineus* (Olivier) (Manachini *et al.*, 2011) and in adults of *Melolontha melolontha* (Brehelin and Zachary, 1986) and *Harmonia axyridis* (Firlej *et al.*, 2012). In the adults of carabids, previous studies showed that plasmatocytes are involved in phagocytosis (Giglio *et al.*, 2008, 2015; Giglio and Giulianini, 2013). However, after artificial non-self challenge with latex beads, granular cells in *H. rufipes* exhibit a high degree of latex bead sequestration. Moreover, the

challenge elicits a change in the relative percentage of hemocyte subpopulations. The number of granular cells increases and they form aggregates, while the reduction of circulating plasmatocytes may be the result of their recruitment in the nodule formation that is a more efficient clearance mechanism for high concentrations of invaders. These findings show that there is a variability among insect taxa in the coordinated response against pathogens involving different subpopulations of hemocytes in phagocytosis

(Hillyer, 2016) because each species modulates the specificity of its immune responses under the selective pressure of its particular environment (Schmid-Hempel, 2005; Siva-Jothy *et al.*, 2005; Sadd and Schmid-Hempel, 2009).

Plasmatic PO and lysozyme-like enzyme activities are two immune markers assayed to evaluate the disease resistance in insects (Adamo, 2004). They are components of the induced response that differ in specificity and are only deployed after an invasive pathogen has been recognized. LPS is a pathogen-associated molecular pattern (PAMP) and triggers proPO activation to provide melanin synthesis that may be involved in several physiological processes, e.g., cuticle sclerotization, wound healing and killing of entrapped parasites or pathogens with a high activating cost for the organism. The challenge with LPS from *E. coli* elicited a significant increase of the basal PO enzyme activity in hemolymph of *H. rufipes*, but it had no significant effect on total PO and lytic activity 24 h after inoculation. Since lysozyme acts mainly on the peptidoglycan, we expected LPS has a moderate effect on lysozyme-like enzyme activity. Because the low number of beetles collected, it lacks mock-injected controls to validate fully our preliminary results. However, previous studies have shown that PO activity displays a dynamic and complex activity after challenges with immune elicitors (Korner and Schmid-Hempel, 2004; Charles and Killian, 2015). Thus, we assume that the low level of total PO recorded in *H. rufipes* may depend on the time post-treatment that the measurements are obtained. Further investigation will clarify if the induction of the systematic proPO cascade may produce through the time several highly reactive (ROS) and toxic compounds that contribute in resistance to pathogens.

In conclusion, our preliminary findings will provide a baseline information for further investigation on pathogen resistance and plasticity in this carabid model. Moreover, the modulation of constitutive and induced immune responses may be used as biomarkers of exposure in an ecotoxicological context.

Acknowledgement

The authors thank Dr Pietro Tarasi (Società Cooperativa Orti dei Monti, Torre Garga Farm) for making fields available for sampling for this study, Dr Antonio Mazzei for the taxonomic identification of species. This work was supported by the Ministero dell'Ambiente e della Tutela del Territorio e del Mare – Ente Parco Nazionale della Sila (Calabria, Italy) (grant no. 2678, XIII/4).

References

Adamo SA. Estimating disease resistance in insects: phenoloxidase and lysozyme-like activity and disease resistance in the cricket *Gryllus texensis*. *J. Insect Physiol.* 50: 209–216, 2004.

Akai H, Sato S. Surface and internal ultrastructure of hemocytes of some insects. In: Gupta AP (ed) *Insect Hemocytes*. Cambridge University

Press, Cambridge, pp 129–154, 1979.

Brehelin M, Zachary D. Insect haemocytes: a new classification to rule out the controversy. In: *Immunity in invertebrates*. Springer, pp 36–48, 1986.

Brygadyrenko VV, Reshetniak DY. Trophic preferences of *Harpalus rufipes* (Coleoptera, Carabidae) with regard to seeds of agricultural crops in conditions of laboratory experiment. *Balt. J. Coleopterol.* 14: 179–190, 2014.

Bulmer MS, Bachelet I, Raman R, Rosengaus RB, Sasisekharan R. Targeting an antimicrobial effector function in insect immunity as a pest control strategy. *Proc. Natl. Acad. Sci.* 106(31): 12652–12657, 2009.

Callewaert L, Michiels CW. Lysozymes in the animal kingdom. *J. Biosci.* 35: 127–160, 2010.

Cavaliere F, Brandmayr P, Giglio A. DNA damage in hemocytes of *Harpalus (Pseudophonus) rufipes* (De Geer, 1774) (Coleoptera, Carabidae) as an indicator of sublethal effects of exposure to herbicides. *Ecol. Indic.* 98: 88–91, 2019.

Cerenius L, Lee BL, Söderhäll K. The proPO-system: pros and cons for its role in invertebrate immunity. *Trends Immunol.* 29: 263–271, 2008.

Charles HM, Killian KA. Response of the insect immune system to three different immune challenges. *J. Insect Physiol.* 81: 97–108, 2015.

Dubovskiy IM, Whitten MMA, Kryukov VY, Yaroslavtseva ON, Grizanov EV, Greig C, *et al.* More than a colour change: insect melanism, disease resistance and fecundity. *Proc. Royal Soc. Lond B: Biol. Sci.* 280(1763): 20130584, 2013.

Firlej A, Girard P-A, Brehélin M, Coderre D, Boivin G. Immune response of *Harmonia axyridis* (Coleoptera: Coccinellidae) supports the enemy release hypothesis in North America. *Ann. Entomol. Soc. Am.* 105(2): 328–338, 2012.

Giglio A, Battistella S, Talarico FF, Brandmayr TZ, Giulianini PG. Circulating hemocytes from larvae and adults of *Carabus (Chaetocarabus) lefebvrei* Dejean 1826 (Coleoptera, Carabidae): Cell types and their role in phagocytosis after in vivo artificial non-self-challenge. *Micron* 39(5): 552–8, 2008.

Giglio A, Brandmayr P, Pasqua T, Angelone T, Battistella S, Giulianini PG. Immune challenges trigger cellular and humoral responses in adults of *Pterostichus melas italicus* (Coleoptera, Carabidae). *Arthropod Struct. Dev.* 44(3): 209–217, 2015.

Giglio A, Giulianini PG. Phenoloxidase activity among developmental stages and pupal cell types of the ground beetle *Carabus (Chaetocarabus) lefebvrei* (Coleoptera, Carabidae). *J. Insect Physiol.* 59(4): 466–74, 2013.

Gillespie and JP, Kanost MR, Trenczek T. Biological mediators of insect immunity. *Annu. Rev. Entomol.* 42: 611–643, 1997.

Giulianini PG, Bertolo F, Battistella S, Amirante GA. Ultrastructure of the hemocytes of *Cetonischema aeruginosa* larvae (Coleoptera, Scarabaeidae): involvement of both

- granulocytes and oenocytoids in in vivo phagocytosis. *Tissue Cell* 35: 243–251, 2003.
- González-Santoyo I, Córdoba-Aguilar A. Phenoloxidase: a key component of the insect immune system. *Entomol. Exp. Appl.* 142: 1–16, 2012.
- Govind S. Innate immunity in *Drosophila*: Pathogens and pathways. *Insect Sci.* 15: 29–43, 2008.
- Gupta AP. *Insect Hemocytes: Development, Forms, Functions and Techniques*. Cambridge University Press, 1979.
- Gupta AP, Sutherland DJ. In vitro transformations of the insect plasmatocyte in some insects. *J. Insect Physiol.* 12: 1369–1375, 1966.
- Hillyer JF. Insect immunology and hematopoiesis. *Dev. Comp. Immunol.* 58: 102–118, 2016.
- Hillyer JF, Strand MR. Mosquito hemocyte-mediated immune responses. *Curr. Opin. Insect Sci.* 3: 14–21, 2014.
- Holland JM. *Carabid beetles: Their ecology, survival and use in agroecosystems. The agroecology of carabid beetles*. Intercept, 2002.
- Honek A, Martinkova Z, Jarosik V. Ground beetles (Carabidae) as seed predators. *Eur. J. Entomol (Czech Republic)*. 100(4): 531-544, 2003.
- Honek A, Martinkova Z, Saska P. Post-dispersal predation of *Taraxacum officinale* (dandelion) seed. *J. Ecol.* 93: 345–352, 2005.
- Honti V, Csordás G, Kurucz É, Márkus R, Andó I. The cell-mediated immunity of *Drosophila melanogaster*: hemocyte lineages, immune compartments, microanatomy and regulation. *Dev. Comp. Immunol.* 42(1): 47–56, 2014.
- Hultmark D. Insect lysozymes. *Exs* 75: 87–102, 1996.
- Hwang S, Bang K, Lee J, Cho S. Circulating hemocytes from larvae of the Japanese rhinoceros beetle *Allomyrina dichotoma* (Linnaeus)(Coleoptera: Scarabaeidae) and the cellular immune response to microorganisms. *PLoS one*. 10(6): e0128519, 2015.
- James RR, Xu J. Mechanisms by which pesticides affect insect immunity. *J. Invertebr. Pathol.* 109: 175–182, 2012.
- King JG, Hillyer JF. Spatial and temporal in vivo analysis of circulating and sessile immune cells in mosquitoes: hemocyte mitosis following infection. *BMC Biology* 11(1): 55, 2013.
- Korner P, Schmid-Hempel P. In vivo dynamics of an immune response in the bumble bee *Bombus terrestris*. *J. Invertebr. Pathol.* 87: 59–66, 2004.
- Lamprou I, Mamali I, Dallas K, Fertakis V, Lampropoulou M, Marmaras VJ. Distinct signalling pathways promote phagocytosis of bacteria, latex beads and lipopolysaccharide in medfly haemocytes. *Immunology* 121(3): 314–327, 2007.
- Lemaitre B, Hoffmann J. The host defense of *Drosophila melanogaster*. *Annu. Rev. Immunol.* 25: 697–743, 2007.
- Manachini B, Arizza V, Parrinello D, Parrinello N. Hemocytes of *Rhynchophorus ferrugineus* (Olivier)(Coleoptera: Curculionidae) and their response to *Saccharomyces cerevisiae* and *Bacillus thuringiensis*. *J. Invertebr. Pathol.* 106: 360–365, 2011.
- Marmaras VJ, Charalambidis ND, Zervas CG. Immune response in insects: the role of phenoloxidase in defense reactions in relation to melanization and sclerotization. *Arch. Insect Biochem. Physiol.*: Published in Collaboration with the Entomological Society of America. 31: 119–133, 1996.
- Marmaras VJ, Lampropoulou M. Regulators and signalling in insect haemocyte immunity. *Cell. Signal.* 21: 186–195, 2009.
- Martins GF, Ramalho-Ortigao JM. Oenocytes in insects. *Inv. Sur. J.* 9(2): 139-152, 2012.
- Miñarro M, Espadaler X, Melero VX, Suárez-Álvarez V. Organic versus conventional management in an apple orchard: Effects of fertilization and tree-row management on ground-dwelling predaceous arthropods. *Agricultural and Forest Entomology* 11: 133–142, 2009.
- Monzó C, Sabater-Muñoz B, Urbaneja A, Castañera P. The ground beetle *Pseudophonus rufipes* revealed as predator of *Ceratitidis capitata* in *Citrus* orchards. *Biol. Control.* 56: 17–21, 2011.
- Moreno-García M, Condé R, Bello-Bedoy R, Lanz-Mendoza H. The damage threshold hypothesis and the immune strategies of insects. *Infect. Genet. Evol.* 24: 25–33, 2014.
- Nappi AJ, Christensen BM. Melanogenesis and associated cytotoxic reactions: applications to insect innate immunity. *Insect Biochem. Mol. Biol.* 35: 443–459, 2005.
- Nappi AJ, Ottaviani E. Cytotoxicity and cytotoxic molecules in invertebrates. *Bioessays*. 22: 469–480, 2000.
- Nappi AJ, Vass E. Cytotoxic reactions associated with insect immunity. In: *Phylogenetic perspectives on the vertebrate immune system*. Springer, pp 329–348, 2001.
- Ottaviani E. Insect immunorecognition. *Inv. Surv. J.* 2: 142–151, 2005.
- Phukan M, Hazarika LK, Barooah M, Puzari KC, Kalita S. Interaction of *Dicladispa armigera* (Coleoptera: Chrysomelidae) haemocytes with *Beauveria bassiana*. *Int. J. Trop. Insect Sci.* 28(2): 88–97, 2008.
- Ratcliffe NA, Rowley AF, Fitzgerald SW, Rhodes CP. Invertebrate immunity: basic concepts and recent advances. In: *Int Rev Cytol.* pp 183–350, 1985.
- Reshetniak DY, Pakhomov OY, Brygadyrenko VV. Possibility of identifying plant components of the diet of *Harpalus rufipes* (Coleoptera, Carabidae) by visual evaluation. *Regulatory Mechanisms in Biosystems*. 3(8) 2017.
- Ribeiro C, Brehélin M. Insect haemocytes: what type of cell is that? *J. Insect Physiol.* 52: 417–429, 2006.
- Rosales C. Phagocytosis, a cellular immune response in insects. *Inv. Surv. J.* 8: 109–131, 2011.
- Sadd BM, Schmid-Hempel P. PERSPECTIVE: principles of ecological immunology. *Evol. Appl.* 2: 113–121, 2009.
- Saska P, Martinkova Z, Honek A. Temperature and rate of seed consumption by ground beetles (Carabidae). *Biol. Control.* 52: 91–95, 2010.
- Saska P, van der Werf W, de Vries E, Westerman PR. Spatial and temporal patterns of carabid

- activity-density in cereals do not explain levels of predation on weed seeds. *Bull. Entomol. Res.* 98: 169–181, 2008.
- Satyavathi V V, Minz A, Nagaraju J. Nodulation: an unexplored cellular defense mechanism in insects. *Cell. Signal.* 26: 1753–1763, 2014.
- Schmid-Hempel P. Evolutionary ecology of insect immune defenses. *Annu. Rev. Entomol.* 50: 529–551, 2005.
- Schmid-Hempel P. Variation in immune defence as a question of evolutionary ecology. *Proc. R. Soc. Lond. B Biol. Sci.* 270: 357–366, 2003.
- Schulenburg H, Kurtz J, Moret Y, Siva-Jothy MT. Introduction. ecological immunology. *Philos Trans. R. Soc. Lond. B Biol. Sci.* 364(1513): 3–14. 2009.
- Siva-Jothy MT, Moret Y, Rolff J. Insect immunity: an evolutionary ecology perspective. *Adv. In. Insect. Phys.* 32: 1–48, 2005.
- Söderhäll K, Cerenius L, Johansson MW. The Prophenoloxidase Activating System and Its Role in Invertebrate Defence. *Ann. N. Y. Acad. Sci.* 712: 155–161, 1994.
- Strand MR. The insect cellular immune response. *Insect sci.* 15: 1–14, 2008.
- Talarico F, Giglio A, Pizzolotto R, Brandmayr P. A synthesis of feeding habits and reproduction rhythm in Italian seed-feeding ground beetles (Coleoptera: Carabidae). *Eur. J. Entomol.* 113: 325–336, 2016.
- Tsakas S, Marmaras VJ. Insect immunity and its signalling: an overview. *Inv. Surv. J.* 7(2): 228–238, 2010.
- Wagner N, Lötters S, Veith M, Viertel B. Effects of an environmentally relevant temporal application scheme of low herbicide concentrations on larvae of two anuran species. *Chemosphere.* 135: 175–181, 2015.
- Wilson K, Cotter SC, Reeson AF, Pell JK. Melanism and disease resistance in insects. *Ecol. Lett.* 4: 637–649, 2001.
- Yamashita M, Iwabuchi K. *Bombyx mori* prohemocyte division and differentiation in individual microcultures. *J. Insect Physiol.* 47: 325–331, 2001.
- Zhao B, Wang MX. Ultrastructural study of the defense reaction against the larvae of *Macracanthorhynchus hirudinaceus* in laboratory-infected beetles. *J. Parasitol.* 70(6): 1098–1101, 1992.